IEEE Access
Multidisciplinary | Rapid Review | Open Access Journal

Received June 30, 2020, accepted July 8, 2020, date of publication July 13, 2020, date of current version July 22, 2020.

Digital Object Identifier 10.1109/ACCESS.2020.3008682

Dual-Channel-Based Mobile Ad Hoc Network Routing Technique for Indoor Disaster Environment

NAMKYU KIM[1], WOONGSOO NA[2], AND SUNGRAE CHO[1], (Member, IEEE)
[1]School of Computer Science and Engineering, Chung-Ang University, Seoul 06974, South Korea
[2]School of Computer Science and Engineering, Kongju National University, Cheonan 31080, South Korea

Corresponding author: Sungrae Cho (srcho@cau.ac.kr)

This work was supported in part by the Chung-Ang University Graduate Research Scholarship in 2019, and in part by the Institute for Information and Communications Technology Promotion (IITP) Grant funded by the Korea Government through the Ministry of Science and ICT (MSIT) (A study on core technology of 5G mobile communication using millimeter wave band) under Grant 2018-0-00889.

ABSTRACT The existing network infrastructure may not work well in a disaster environment caused by a fire or an earthquake. Instead of relying on the existing infrastructure, communicating through a mobile ad hoc network (MANET) is recommended because MANET can configure a network without an infrastructured communication system. In addition, firefighters conducting emergency activities in harsh environments surrounded by flames and smoke need a communication system to assist their rapid firefighting operations. Existing work is not suitable for indoor firefighter communications because they did not consider the indoor disaster environment well. In this proposed scheme, dual channels (i.e., 2.4 GHz and sub-GHz bands) are used for an efficient routing table configuration. Data frame and HELLO message are exchanged through the 2.4 GHz band, while the neighbor list of each node is exchanged through the sub-GHz band. Each node can configure the routing table based on the exchanged neighbor list. A performance evaluation is conducted to compare the proposed technique with enhanced versions of optimized link state routing (OLSR) and destination-sequenced distance vector routing (DSDV). The results show that the proposed scheme outperforms the other two MANET routing algorithms (i.e., OLSR-mod and DSDV-mod) in terms of the packet delivery ratio (PDR), end-to-end delay, and initial routing table configuration time approximately 27.8%, 4.7%, and 166.7%, respectively.

INDEX TERMS Mobile ad hoc network, indoor disaster environment, dual channel, firefighter communication.

I. INTRODUCTION

Adisaster environment caused by a fire or an earthquake are very dangerous due to fire, smoke and broken building or obstacle. Firefighters try to rescue people as soon as possible to save lives in disaster area. For this reason, a communication system for firefighters is essential for rapid firefighting operations. In addition, stable communications is required to support firefighting operations. Since existing network infrastructure is highly likely to be broken by disaster, we cannot stick to infrastructure network system in indoor disaster environments. Mobile Ad hoc Network (MANET) is a promising solution because it does not require infrastructure network system. Nodes can configure own network by themselves. This paper proposes a dual-channel-based MANET routing (DCR) technique for an indoor disaster environment. In the proposed technique, the location information is obtained using an indoor positioning system, and 2.4 GHz and sub-GHz channels are used.

The associate editor coordinating the review of this manuscript and approving it for publication was Ding Xu.

A. RELATED WORK

Two kinds of MANET protocols are dominantly used: proactive and reactive protocols. While proactive protocols, such as optimized link state routing (OLSR) [1], construct the routing table in advance, reactive protocols, such as ad-hoc on-demand distance vector routing (AODV) [2], process route search whenever a packet delivery is required. Location-aided routing (LAR) and greedy perimeter stateless

routing (GPSR) are representative routing algorithms based on location information [3], [4]. LAR is an algorithm that broadcasts only within a limited area using the physical location information of the source and destination nodes. All nodes in the network assume that they know their physical location using a global positioning system (GPS). LAR is based on dynamic source routing (DSR) and defines expected and request zones between the source and destination nodes, but, LAR is not a feasible solution because nodes are located indoors, where GPS positioning is not possible. Meanwhile, GPSR, based on the location information, uses the physical location information of its own to select the closest node to the destination among the nodes in its transmission range and transmit the data. Therefore, this protocol can provide the shortest path between the source and destination nodes. However, GPSR has the disadvantage of being unable to search for the route in the presence of a void zone, which is a blind spot where routing cannot be done, because of a large overhead when maintaining the location registration database. Many researchers have also studied enhanced versions of existing MANET routing protocols such as OLSR, AODV, and DSR. Anand *et al*. proposed routing protocol based on AODV [5]. The proposed protocol uses the distance between nodes calculated from the received signal strength indicator. However, this routing algorithm may not work well in indoor disaster area, because the distance could be calculated wrong by obstacles. An improved scheme for OLSR was proposed in [6]. Since the mobility of nodes did not considered in multipoint relay (MPR) selection from OLSR, this paper tried to select MPR nodes as most static nodes to reduce the packet loss ratio. Al-Zahrani analyzed the existing flooding algorithms for routing, and classified them into four types: traditional flooding, time-to-live (TTL) based expanding ring search flooding scheme, TTL-based scope routing flooding, and multi-point relays flooding [7]. Enhancement algorithms are suggested based on the analysis of each flooding class to minimize the cost based on energy and time consumptions, with improvements in search set values and intervals of routing algorithms. The modified versions of each routing algorithm showed better performances in terms of the throughput, end-to-end delay, and routing overhead. However, these algorithms are not suitable for indoor firefighter communication because deployed environment did not consider obstacles.

Many studies were conducted for the communication in the disaster area. Cabrero *et al*. [8] investigated the traces of firefighters in wildfires. They analyzed the pattern of firefighter communications in wildfires and found that a large buffer size is important. In their study, communication equipment was installed in the vehicle, and the environment was an outdoor environment; hence, the application fields are far from those in our study. An emergency ad hoc networks by using drone mounted base stations were proposed in [9]. Long term evolution femtocell base station is mounted on the drone. Necessary amount of drones are dispatched to the disaster area to satisfy the bit rate required by users. Similarly, delay tolerant routing protocol in unmanned aerial vehicle (UAV) networks for post-disaster operation was proposed in [10]. The proposed scheme estimated the future UAV locations based on location and speed information. The UAV node decided whether to forward or not based on the location prediction. Since most studies for routing in the disaster area assumed an outdoor disaster environment, they are not suitable for the indoor disaster area.

Many researchers have also studied communication techniques using multiple wireless channels to achieve energy-efficient communication. A dual-band (2.4 GHz and 868 MHz) ultra-low-power wake-up radio receiver was proposed in [11]. This proposed technique increased the flexibility of the wake-up radio and allowed interoperability with the 2.4 GHz and 868 MHz bands. The experimental result provided that the proposed technique improves performance in terms of power consumption and receive sensitivity. Routing methods in multi-radio mesh network are considered in [12], [13]. A re-configuration optimization model was proposed in [12], which tried to optimize the network throughput in addition to reducing the disruption to the mesh clients' traffic due to the re-configuration process. However, those papers considered communication flows from the gateway to the mesh clients only. Moreover, these methods did not consider the mobility well; hence, they are not suitable for the firefighter communication.

Many low-power communication techniques for Internet of Things devices on the sub-GHz band have been studied and developed. Long range (LoRa), which is a type of low power wide area network (LPWAN) technology, can transmit far distances with low power [14], [15]. LoRa uses an unlicensed spectrum such as 433 MHz, 868 MHz, 915 MHz, and 923 MHz. Meanwhile, ZigBee, which is based on the 802.15.4 standard, is a communication specification used for a small-sized low power network [16]. ZigBee operates on the 868 MHz, 915 MHz, and 2.4 GHz unlicensed bands. These sub-GHz technologies aim to achieve low-energy and data rate communication with a narrow frequency band. The data rate of the sub-GHz band is small for usage in actual data communication, but a small frame, such as a simple control message can be sufficiently exchanged through the sub-GHz band.

Positioning systems for indoor environments have been developed. The personal dead-reckoning system is a positioning system that measures and tracks the location of a walking person for GPS-denied environments [17]. Inertial measurement units (IMUs) are attached to the boots such that the position of each user can be measured. A real-time cooperative localization system utilizing dual foot-mounted inertial sensors and inter-agent ranging was presented in [18]. This system can help firefighters do rapid firefighting operations in an indoor disaster area. A framework for accurate trajectory-tracking using the deep learning method was proposed in [19]. The framework could learn and reconstruct pedestrian trajectories from raw IMU data. The firefighter's real-time location information can be used not only to determine the current location of a firefighter in a building

but also to calculate the routing link costs. The proposed study adopts the indoor positing system to calculate the link cost.

B. MOTIVATION

Existing work on routing protocols for MANET or wireless mesh network is not suitable for indoor firefighting communications. The reasons are as follows:

- The mobility of nodes is not provided, or is not considered properly during routing process.
- The existing routing protocols are not suitable for indoor communication, because they require the GPS data or infrastructure for communication.
- The end-to-end delay is too long to use in emergency scenario.
- Obstacles are not considered from communication scenario, so that communications in indoor disaster area with obstacles (i.e., walls, broken building and the furniture) may not work well.

Therefore, the routing protocol for indoor firefighter communication in indoor disaster area is required.

C. CONTRIBUTION

The contributions of this paper are as follows:

- A novel MANET routing scheme is proposed using the 2.4 GHz and sub-GHz bands, which are frequently-used unlicensed bands. The proposed scheme uses the 2.4 GHz to exchange data frame and HELLO message, and uses sub-GHz for exchanging NEIGHBORS message. Each node can discover one-hop neighbors and calculate the link cost by exchanging HELLO message. The routing table is configured fast, because the link state of each node is exchanged through sub-GHz band with a large coverage, which is important for emergency rescue. In addition, the overhead in the 2.4 GHz band can be reduced by transmitting part of the control frame through the sub-GHz band.
- A novel routing-cost calculation is proposed. The routing cost is a sum of link costs in the route. The link cost is calculated with SNR and the position of the nodes. DCR is suitable at indoor firefighter communication because the SNR and mobility of each node are considered at the routing-cost calculation.
- A performance evaluation, which compares the performance of the proposed scheme to those of the enhanced versions of OLSR and the destination-sequenced distance vector routing (DSDV), namely OLSR-mod and DSDV-mod, is conducted. The performance evaluation shows that the proposed scheme outperforms OLSR-mod and DSDV-mod in terms of packet delivery ratio (PDR), end-to-end delay, and initial routing table configuration time. The PDR of DCR is at least 9.8% higher than that of OLSR, and at least 27.8% higher than that of DSDV. The end-to-end delay of DCR is similar to or smaller than that of OLSR and DSDV. Moreover, the end-to-end delay of DCR is always less than 10 ms. DCR takes 3 s to configure the initial routing table, while the other two routing protocols take more than 8 s.

The remainder of this paper is organized as follows: Section II analyzes the application field; Section III introduces the novel dual-channel-based mobile ad hoc routing technique; Section IV discusses the evaluation performance of our proposed algorithm with an ns-3 simulation tool; and finally, we draw the conclusions in Section V.

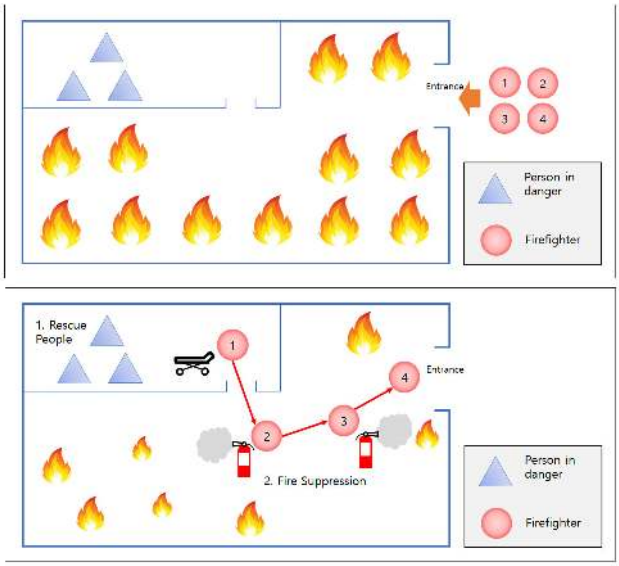

FIGURE 1. Scenario of indoor firefighters' emergency rescue activities.

II. SYSTEM MODEL AND BASIC ASSUMPTIONS

A. INDOOR FIREFIGHTER COMMUNICATION SCENARIO

In this subsection, the communication scenario among firefighters in the indoor disaster area is described, and the communication environment is analyzed. The proposed routing technique was devised for firefighter communication at indoor disaster environment. Fig. 1 shows a example of firefighters' emergency rescue activities. Firefighters try to rescue people and extinguish a fire as soon as possible. However, in a disaster environment, fire, smoke, and broken obstacles limit cognitive sensations, such as hearing, sight, and smell. In addition, firefighters are equipped with firefighting suits and heavy equipment for rescue operations. Therefore, it is highly likely that a normal voice conversation is impossible. From the bottom figure of Fig. 1, node(firefighter) 4 discovers people in danger at the room and tries to request support to node 1 who is near the entrance. Because distance between node 1 and node 4 is too far to communicate directly, the request data must be delivered through node 2 and node 3. Therefore, we need a routing algorithm which can forward the data to the destination correctly. From this scenario, the indoor firefighter communication environment can be analyzed as follows:

- First, this network is a sparse network with a few nodes (i.e., firefighters), which are maintaining a

certain distance. The number of one-hop neighbors of a node does not exceed 10.
- Second, it is a low mobility MANET environment. Firefighters have very slow movements because they perform rescue operations and extinguish fires with heavy equipment. Moving in the disaster area may be difficult due to fire and smoke. Therefore, the node speed is assumed to not exceed 5 m/s, which is similar to the running speed of marathon runners.
- Third, the nodes of the same network exist within the coverage of the sub-GHz band communication.

Therefore, the proposed algorithm should minimize the delay of frames transmitted, provide fast route configuration, and be robust against a harsh environment caused by high temperature and obstacles.

III. DUAL-CHANNEL-BASED ROUTING SCHEME

A. GOAL OF THE ALGORITHM

The goal of the proposed algorithm is to achieve the following:

1) Low delay: the data that the firefighters transmit and receive are voice, images, and videos, which are time-sensitive. A high delay can lead to a fatal accident related to the firefighter communication in the disaster area.
2) High PDR: similarly, a high PDR is very important. Firefighters should perform their missions as quickly as possible through continuous communications. These communications include commands and real-time reporting.
3) Fast routing table configuration: firefighters should perform missions, such as firefighting and emergency rescue, as soon as they arrive at the emergency site. Therefore, a long time taken to construct a routing table will greatly impede firefighters from performing their duties.

We attempted to accomplish a low delay, high PDR, and fast routing table configuration speed by proposing our own routing scheme.

B. CHARACTERISTICS OF THE ALGORITHM

The algorithm characteristics determined according to the application field analysis are presented below.

TABLE 1. Characteristics of the routing algorithm.

Characteristic	Reason
Proactive	Each node has low mobility; hence, the topology does not change often.
Link-state	The transmission of the radio waves is restricted due to obstacles; hence, link-state routing is more suitable for the application field and collecting information on the surrounding links from the sub-GHz channel is easy.
Table-driven	The number of nodes is small; hence, there is little overhead for maintaining the table, and it is efficient for performing the MANET routing in a table-driven manner.

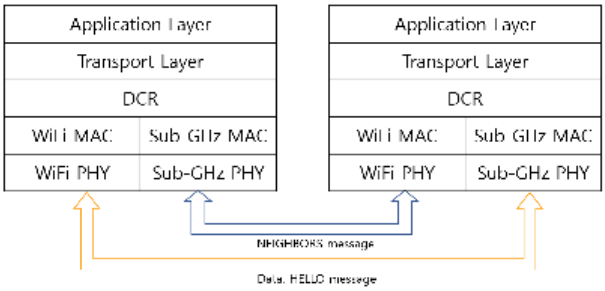

FIGURE 2. Communication architecture of the DCR scheme. Architecture model is based on TCP/IP 5 layer model.

C. COMMUNICATION ARCHITECTURE

Fig. 2 illustrates the communication architecture of the DCR. DCR is located in the network layer. Like existing routing protocol, DCR determines the route for the destination and forward the packet. To configure the routing table, DCR transmits HELLO and NEIGHBORS message periodically. Data frame and HELLO message are transmitted over the 2.4 GHz band, while NEIGHBORS frame is transmitted over the sub-GHz band.

D. ROUTING ALGORITHM

The data structures of the routing scheme are described in Table 2.

TABLE 2. Data structures of the routing algorithm.

Data structure	Explanation
Neighbor table	Neighbor table consists of neighbor entries. Each entry contains the IP address of the neighbor and edge cost between own node and the neighbor. The entry is updated whenever the node receives the HELLO message.
Routing table	Routing table consists of routing table entries. Each routing table entry contains the IP address of the destination, one-hop route, two-hop route, and route cost, which is a sum of the link costs. Routing table is updated whenever the topology graph is updated.
Topology graph	Topology graph is a set of wireless link (edge) states between nodes. Each wireless link state contains the IP address of sender, IP address of receiver, and edge cost. Topology graph is updated whenever the node receives the NEIGHBORS message.
HELLO interval (t_H)	Each node transmits HELLO message every t_H seconds.
NEIGHBORS interval (t_N)	Each node transmits NEIGHBORS message every t_N seconds.

Algorithm 1 and the state diagram of Fig. 3 describe how DCR operates. t_H^{prev} and t_N^{prev} denote the previous transmitting time of HELLO and NEIGHBORS messages, respectively. A loop from lines 2 to 28 is repeated until the firefighting operation ends. HELLO and NEIGHBORS messages are transmitted every t_H and t_N, respectively (lines 4 to 11). Fig. 4 shows the HELLO message. Each node transmits the HELLO message for every Hello interval (t_H). The HELLO message

Algorithm 1 Pseudo Code of DCR

1: **initialize:** $t_H^{prev} = 0, t_N^{prev} = 0$
2: **while** *true* **do**
3: $t^{cur} =$ CurrentTime
4: **if** $t^{cur} > t_H^{prev} + t_H$ **then**
5: Transmit HELLO message
6: $t_H^{prev} = t^{cur}$
7: **end if**
8: **if** $t^{cur} > t_N^{prev} + t_N$ **then**
9: Transmit NEIGHBORS message
10: $t_N^{prev} = t^{cur}$
11: **end if**
12: **if** HELLO message is received from WiFi channel **then**
13: Update neighbor table
14: **end if**
15: **if** NEIGHBORS message is received from sub-GHz channel **then**
16: Update topology graph
17: Update routing table
18: **end if**
19: **if** data frame is queued **then**
20: Find next-hop from the routing table
21: **if** transmitting to next-hop is available **then**
22: Forward to next-hop
23: **else**
24: Operate Route Recovery
25: Forward to next-hop
26: **end if**
27: **end if**
28: **end while**

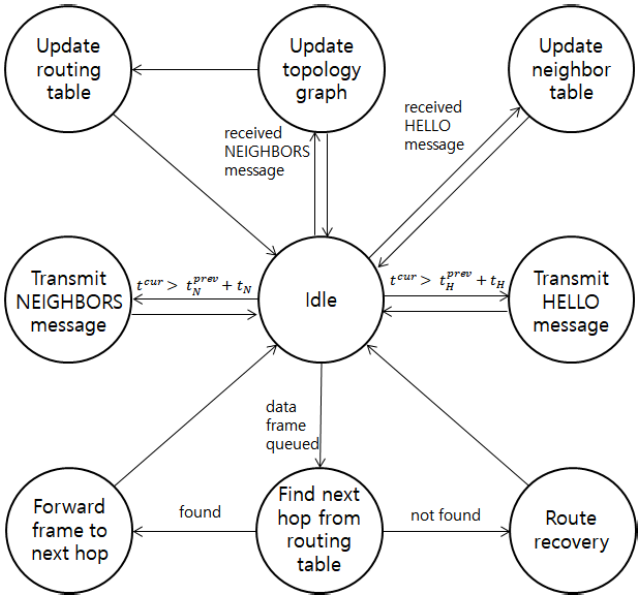

FIGURE 3. State diagram of DCR.

contains the position of the sender. A node that receives the HELLO message updates or adds the corresponding entry

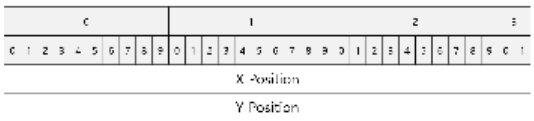

FIGURE 4. HELLO message.

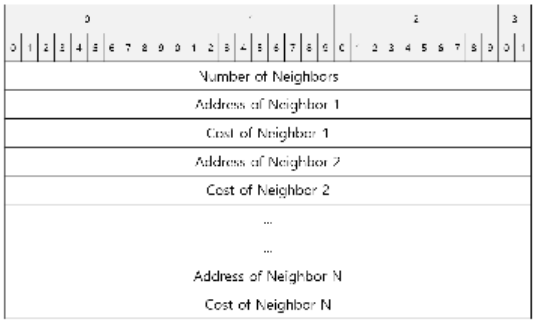

FIGURE 5. NEIGHBORS message.

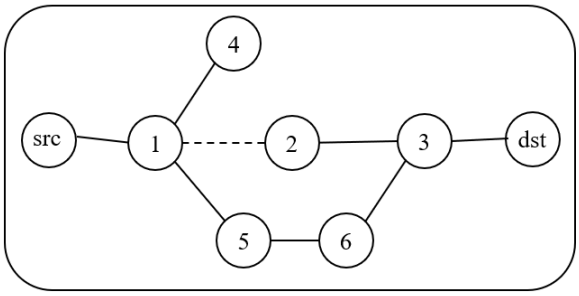

FIGURE 6. Example of route recovery.

of the neighbor table (lines 12 to 14). Each neighbor table entry contains address of the neighbor, edge cost, and the expiration time. The edge cost calculation is explained in the next subsection. The expiration time is calculated as $t^{cur}+d_N$, where t^{cur} denotes the current time, and d_N denotes the duration of the neighbor table entry. The corresponding entry will be removed if the expiration time is not updated, and the current time has passed that expiration time. Fig. 5 shows the NEIGHBORS message. First, the number of neighbors is provided to decode the NEIGHBORS message with the exact size. The address of neighbor and cost of neighbor are then provided for each neighbor of the sender. A node that receives the NEIGHBORS message updates the topology graph which is a set of edges (lines 15 to 18). The routing table is updated using Dijkstra's algorithm after the topology graph is updated. If the number of neighbors is 10, the size of the NEIGHBORS message, including the WiFi header is 144 bytes, and the data rate is 1.125 Kbps if $t_N = 1$ s. Therefore, communicating through the sub-GHz band, which has a low data rate, is quite feasible.

DCR finds the route from the routing table (lines 19 to 20) when the data frame is queued. The data frame is forwarded according to the table entry (lines 21 to 22) if the corresponding entry exists in the routing table. Meanwhile, a fast

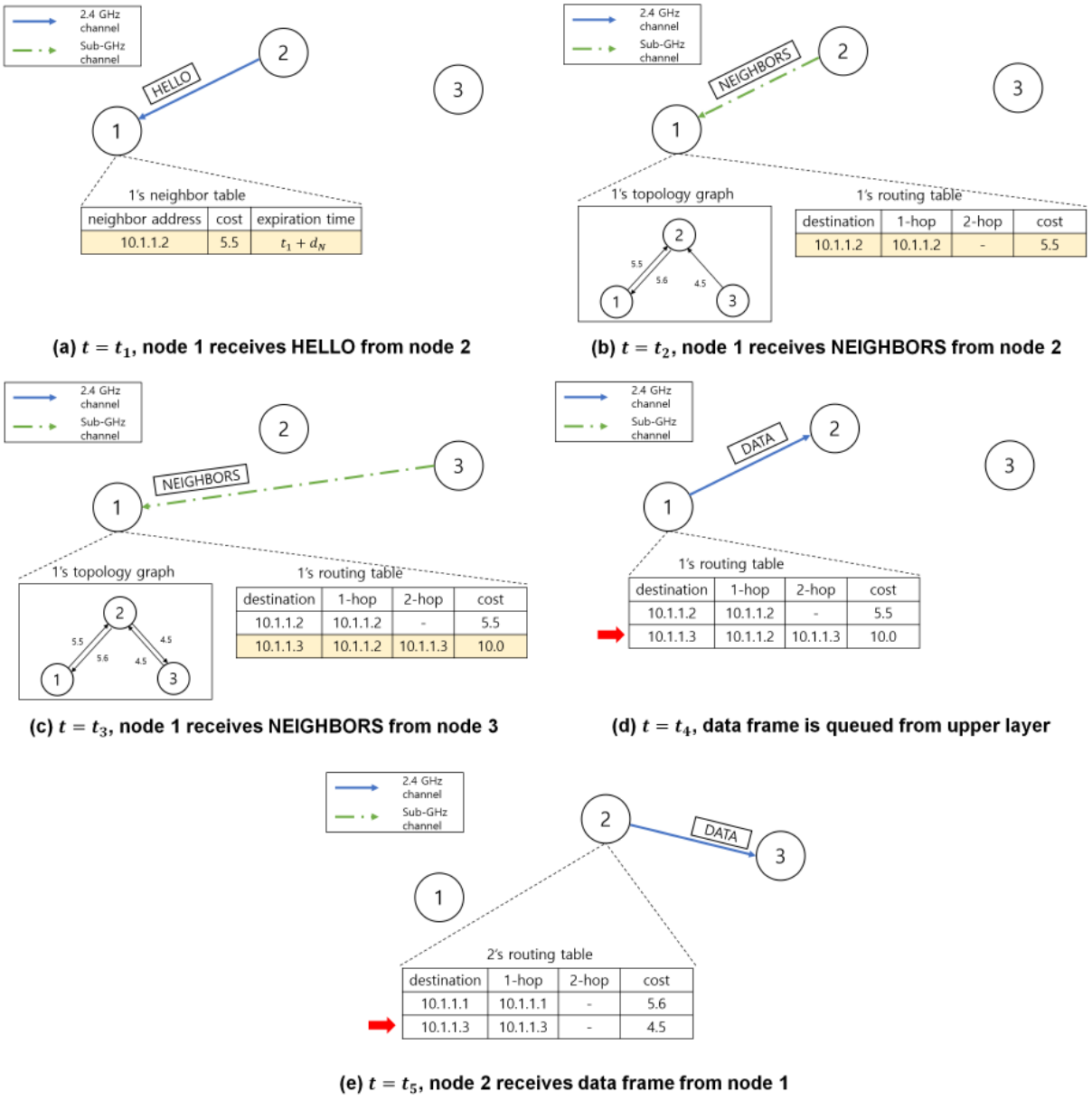

(a) $t = t_1$, node 1 receives HELLO from node 2

(b) $t = t_2$, node 1 receives NEIGHBORS from node 2

(c) $t = t_3$, node 1 receives NEIGHBORS from node 3

(d) $t = t_4$, data frame is queued from upper layer

(e) $t = t_5$, node 2 receives data frame from node 1

FIGURE 7. Routing and forwarding process.

routing-recovery system is used if the route does not exist (lines 23 to 26). While the frame is being delivered from the source node to the destination node, a link on the routing path can be disconnected. In preparation for this situation, each node calculates the two-hop route node for each destination node and finds the route to the two-hop route node. In Fig. 6, for example, the source node (src) transmits the data to the destination node (dst). The data frame arrives at node 1. The one-hop node is node 2 and two-hop node is node 3 according to the routing table of the node 1. However, the link between node 1 and node 2 is disconnected. The route recovery system then operates. Node 1 tries to find the route to node 3 which is a two-hop route node. Assume that the new route is (1, 5, 6, 3). The packet is then forwarded through the new route. Dijkstra's algorithm is operated for all nodes in the topology graph if the route is not found.

Fig. 7 shows the routing and forwarding processes of DCR. Assume that there are 3 nodes: node 1, node 2, and node 3. Addresses of nodes are from 10.1.1.1 to 10.1.1.3. Node 2 can communicate to node 1 and node 2 directly through 2.4 GHz channel. However, node 1 and node 3 can communicate each other only through node 2 over 2.4 GHz channel. When $t = t_1$, node 1 receives the HELLO message from node 2 (Fig. 7(a)). Node 1 updates the neighbor table by adding the new entry for the node 2. When $t = t_2$, node 1 receives NEIGHBORS message from node 2 (Fig. 7(b)). Node 1 updates the topology graph and the routing table. The topology graph is a set of directed edges. The routing

table is updated using Dijkstra's algorithm with the topology graph. Similarly, when $t = t_3$, node 1 updates the topology graph and the routing table after node 1 receives the NEIGHBORS message from node 3 (Fig. 7(c)). Node 1 can receive the NEIGHBORS message from node 3 because the NEIGHBORS message is transmitted through sub-GHz channel. Now, node 1 has routing entries destined to node 2 and node 3. When $t = t_4$, the data frame destined to node 3 (10.1.1.3) is queued from upper layer at node 1 (Fig. 7(d). Because node 1 has the routing entry destined to node 3, node 1 forwards the data frame to node 2 according to the routing entry. When $t = t_5$, node 2 receives the data frame from node 1 (Fig. 7(e)). Node 2 forwards the data frame to node 3 according to its routing table (assuming that node 2 already configured own routing table).

E. ROUTING COST CALCULATION

This subsection describes the calculation of routing cost of the proposed algorithm. The routing cost is a sum of all costs in the route. Routing cost $C(i, j)$ from nodes i to j is given by

$$C(i,j) = \sum_{l \in R_{i,j}} c(l) \tag{1}$$

where $c(l)$ is a cost of the link l. We proposed two types of link cost: 1) using SNR and 2) using SNR, position information and moving speed. The algorithm choose one of them depending on the environment. The link cost using SNR from the node i to the node j is given by

$$c(i,j) = \begin{cases} \dfrac{\rho}{1 - E_F\left(\frac{E_b}{N_0}\right)} & \text{if } E_F\left(\dfrac{E_b}{N_0}\right) \geq E_t \\ \dfrac{1}{1 - E_F\left(\frac{E_b}{N_0}\right)} & \text{if } E_F\left(\dfrac{E_b}{N_0}\right) < E_t \end{cases} \tag{2}$$

where ρ is a penalty weight such that $\rho > 1$, and E_t is a link error threshold. $E_F\left(\frac{E_b}{N_0}\right)$ is a frame error rate, which is given by

$$E_F\left(\frac{E_b}{N_0}\right) = 1 - \left(1 - E_B\left(\frac{E_b}{N_0}\right)\right)^L \tag{3}$$

where L is a length of frame in bit, and $E_B\left(\frac{E_b}{N_0}\right)$ is a bit error rate, which is determined by the modulation scheme [20]–[23]. $\frac{E_b}{N_0}$ is calculated from the bandwidth W, data rate R, and SNR as

$$\frac{E_b}{N_0} = \frac{W}{R} \times \text{SNR}. \tag{4}$$

$\vec{p} = (p_x, p_y), \vec{v} = (v_x, v_y)$ denote relative position vector, and relative velocity vector of the neighbor from own node, respectively. $\vec{p}$ and $\vec{v}$ can be calculated easily from the HELLO message and own position information. A node escape time t_e, which is the time required for the distance between two nodes to reach the maximum transmission distance r_t, is formulated as

$$\|\vec{p} + t_e\vec{v}\| = r_t. \tag{5}$$

Equation (5) is rewritten as

$$\|(p_x + t_e v_x, p_y + t_e v_y)\| = r_t \tag{6}$$

which leads to

$$t_e = \frac{-(p_x v_x + p_y v_y) + \sqrt{(p_x v_x + p_y v_y)^2 - X}}{v_x^2 + v_y^2} \tag{7}$$

where $X = (v_x^2 + v_y^2)(p_x^2 + p_y^2 - r_t^2)$. The cost using the SNR, position information, and moving speed from the node i to the node j is given by

$$c(i,j) = \begin{cases} \dfrac{\rho \times (1 + \max(0, d_N - t_e))}{1 - E_F\left(\frac{E_b}{N_0}\right)} & \text{if } E_F\left(\dfrac{E_b}{N_0}\right) \geq E_t \\ \dfrac{1 + \max(0, d_N - t_e)}{1 - E_F\left(\frac{E_b}{N_0}\right)} & \text{if } E_F\left(\dfrac{E_b}{N_0}\right) < E_t \end{cases} \tag{8}$$

When $t_e < d_N$, the link cost increases with decreasing t_e; hence, the link that is more likely to be disconnected, has a larger cost.

IV. PERFORMANCE EVALUATION

This section discusses the performance evaluation to verify the proposed technique. The algorithm was implemented with the ns-3 network simulator based on C++ language. The proposed algorithm was compared with two proactive routing protocols, namely OLSR-mod and DSDV-mod, which are enhancement version of two proactive MANET protocols, OLSR and DSDV [7]. The following experiments were conducted:

- Experiments without mobility were first conducted. DCR was compared with OLSR-mod and DSDV-mod over the data rate of the source node to show the effect of a simple and lightweight control message exchange method through sub-GHz. We then compared the initial throughput of DCR, OLSR-mod, and DSDV-mod during the first 30 s to see how quickly the routing table is constructed.
- Experiments with mobility were conducted. Three routing protocols were compared with different speeds in terms of the PDR and the end-to-end delay to analyze how the proposed scheme is tolerable to mobility. A comparison over the number of nodes was also performed for a comparison according to the network size.
- Experiments were performed with different transmission HELLO and NEIGHBORS message intervals for DCR to obtain an intuition about how the interval between transmitting the HELLO and NEIGHBORS messages affects the performance.

Fig. 8 shows the simulation space. The size of the simulation space was 80 m × 80 m. Each node was randomly deployed on the space. The size of each room was 20 m × 20 m. To consider the obstacle model, we used building topology. Four rooms were located at the top, other four rooms were

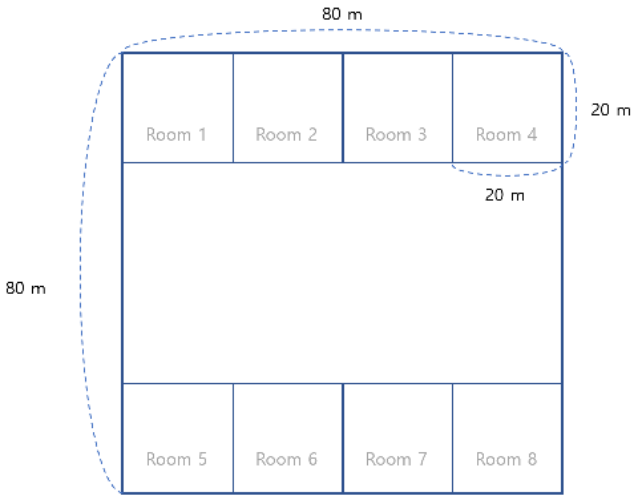

FIGURE 8. Simulation map.

TABLE 3. Simulation parameters.

Simulation parameter	Value
Transmit power	15 dBm
Receive sensitivity	−51 dBm
The number of nodes	{10, 15, 20, 25, 30}
Maximum speed	{1, 2, 3, 4, 5} (m/s)
Packet size	1024 bytes
Hello interval (t_H)	1 s
Neighbor interval (t_N)	1 s
Neighbor entry duration (d_N)	2 s
Maximum transmission distance (r_t)	22 m
Penalty weight (ρ)	10
Simulation time	600 s

located at the bottom. A building propagation loss model was used; hence, the loss increased if the wall was between the transmitter and the receiver. A random seed was fixed at the same simulation; hence, the node position was the same for all three algorithms. The random seed was changed for each experiment. The DCR, OLSR-mod, and DSDV-mod shared the random seed for the same experiment. Table 3 lists the simulation parameters. The transmit power and receive sensitivity were set to 15 dBm and −51 dBm, respectively. A stable communication is available if the distance between the nodes is less than 20 m and there was no wall between the transmitter and the receiver. Communication is almost impossible if the distance exceeds 22 m.

A. COMPARISON WITH OLSR-MOD AND DSDV-MOD

1) EXPERIMENTS WITHOUT MOBILITY

DCR was compared with OLSR-mod and DSDV-mod at the fixed-position scenario. Fig. 9 shows the PDR of each MANET algorithm with varying data rate of the source node. For the fixed scenario, packets were sent only if the route existed. DCR outperformed the other two algorithms in terms of PDR for two reasons: first, the DCR nodes exchange their topologies using the sub-GHz; hence, they can save the WiFi channel resource to maintain the routing table when compared to the other two algorithms; second, the routing

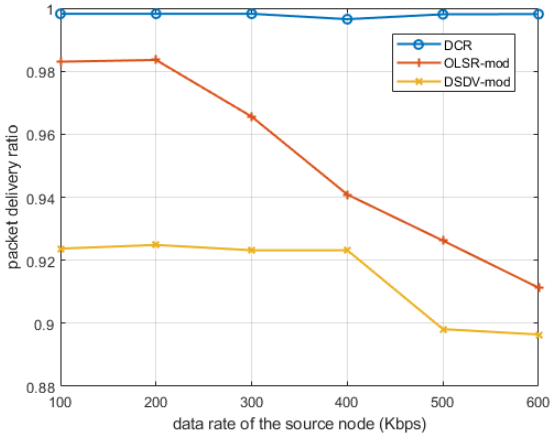

FIGURE 9. PDR over data rate of the source node with a fixed location.

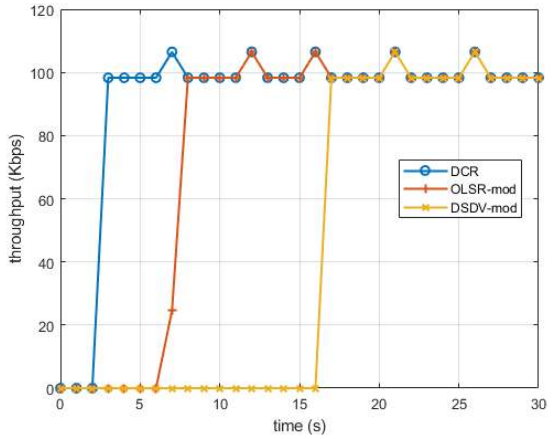

FIGURE 10. Throughput for the first 30 s.

table is configured faster than the other algorithms as the link information is transmitted far through the sub-GHz channel. This effect is evident in Fig. 10. Fig. 10 shows the throughput in Kbps per second during the first 30 s. DCR can configure the routing table faster than the other two algorithms. The routing table configuration times of DCR, OLSR-mod, and DSDV-mod are 3 s, 8 s, 17 s, respectively. The routing table was quickly constructed through the sub-GHz band; thus, the routing table configuration time was shorter than those of the other algorithms. This is especially important because firefighters are required to rescue people as soon as they enter the disaster environment.

2) COMPARISON OVER MAXIMUM SPEED

Experiments were conducted with mobility. Each node moved with a random waypoint mobility model and repeatedly moved to a random point on the simulation plane. The number of nodes was 25. The number of source and destination nodes was 3. The data rate of each source node was 10 Kbps. The speed was set to a random value in range [0, MaxSpeed]. The maximum speed of nodes varied from 1 to 5 m/s. Given that firefighters are wearing firefighter suits and special equipment, 5 m/s (i.e., 18 km/s) is very

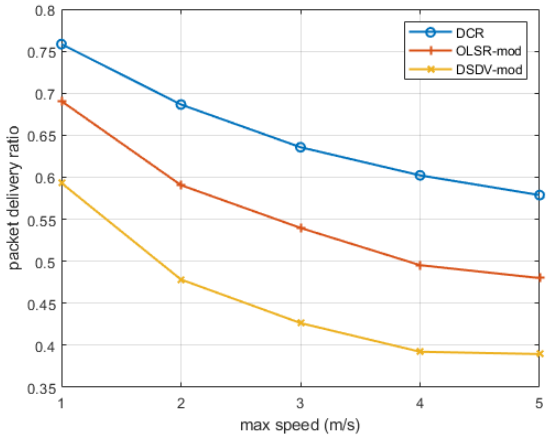

FIGURE 11. PDR over maximum speed.

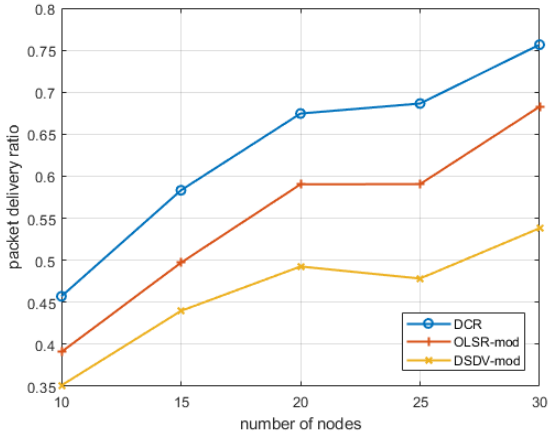

FIGURE 13. PDR over the number of nodes.

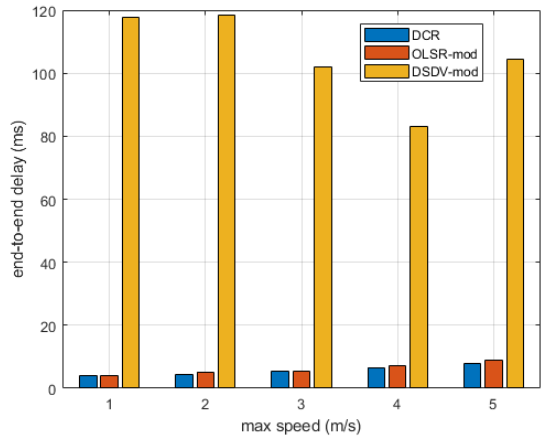

FIGURE 12. End-to-end delay over maximum speed.

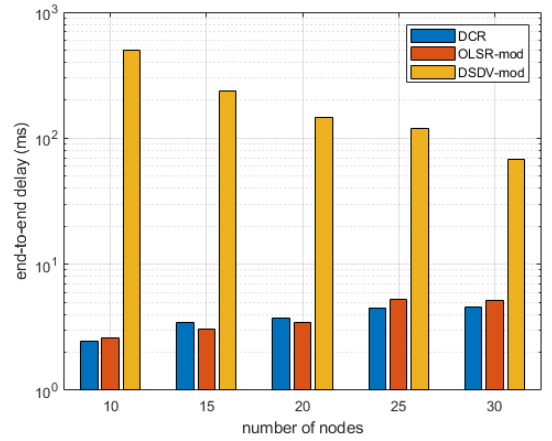

FIGURE 14. End-to-end delay over the number of nodes. A logarithmic scale is adapted on y-axis (end-to-end delay).

TABLE 4. Standard deviation of the comparison over maximum speed.

speed (m/s)		1	2	3	4	5
DCR	PDR	0.0725	0.0621	0.0617	0.0598	0.0711
	delay	0.0006	0.0010	0.0019	0.0024	0.0038
OLSR-mod	PDR	0.0835	0.0739	0.0750	0.0782	0.0876
	delay	0.0010	0.0016	0.0023	0.0039	0.0044
DSDV-mod	PDR	0.0790	0.0672	0.0569	0.0799	0.0725
	delay	0.0819	0.0873	0.0698	0.0581	0.0768

fast. Other simulation parameters are specified in the table 3. Figs. 11, 12, and Table 4 show the experimental results of the three protocols over maximum speed of the nodes. The goal of these experiments was to analyze the DCR performance with environments of various speeds of firefighters. Fig. 11 depicts that the PDR decreased with the increasing speed. The links of each node more frequently changed because of high mobility as the speed of nodes increased. The PDR decreased because the routing table did not properly reflect the changed link state. In terms of the PDR, DCR outperformed OLSR-mod and DSDV-mod for every case. The PDR of DCR was 0.067(9.8%) higher than that of OLSR-mod and 0.165(27.8%) higher than that of DSDV-mod when the maximum speed was 1 m/s. In addition, the differences of the PDR between DCR and the other routing protocols increased.

Fig. 12 shows the end-to-end delay of each routing algorithm over maximum speed. The delay of DSDV-mod was much higher than those of the other two algorithms because DSDV-mod improved PDR through packet buffering. Nevertheless, the PDR of DSDV-mod was much lower than that of DCR. Retransmissions could occur because the routing table does not reflect the current link state or link state changes, while the packet is being transferred from the source node to the destination node. The end-to-end delays of both DCR and OLSR-mod increased with the increasing maximum speeds. Nevertheless, the end-to-end delay was very small (i.e., less than 10 ms); thus, no disruption existed in smooth communication between firefighters. Table 4 shows the standard deviation of each routing algorithm over maximum speed. The standard deviation of PDR was large for three routing protocols because the PDR varied significantly as the locations of nodes changed. Nevertheless, the standard deviation for PDR of DCR is smaller than those of OLSR-mod and DSDV-mod, which means that the DCR shows robust performance than the others. Consequently, DCR showed great performance in terms of high mobility compared to OLSR-mod and DSDV-mod.

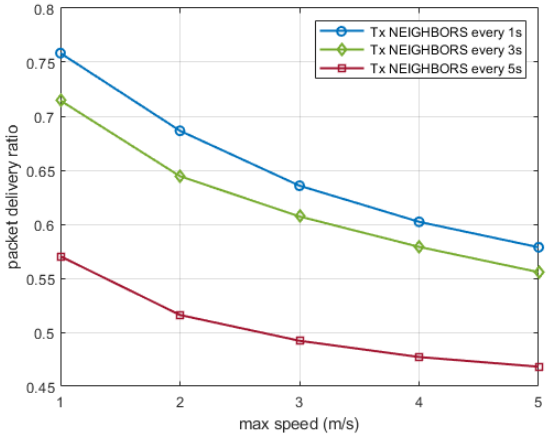

FIGURE 15. PDR for NEIGHBORS message interval over maximum speed.

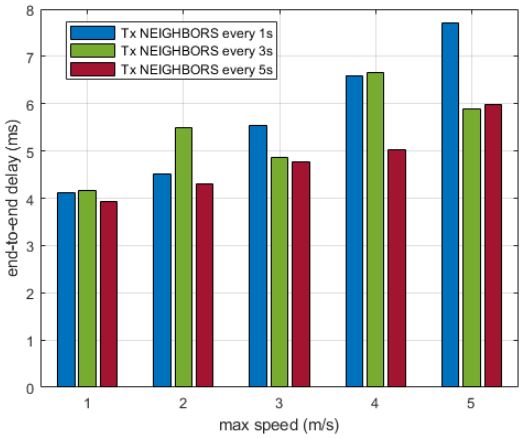

FIGURE 16. End-to-end delay for NEIGHBORS message interval over maximum speed.

3) COMPARISON OVER THE NUMBER OF NODES

Experiments were conducted with the varying number of nodes. The experimental results over the number of nodes are presented in Figs. 13 and 14. The goal of these experiments was to analyze the performance of DCR from small network (10 nodes) as well as a large network (30 nodes). The number of nodes varied from 10 to 30. The number of source and destination nodes was 3. The maximum speed was set to 2 m/s. The data rate was set to 10 Kbps. Other simulation parameters are same as those of subsection IV-A2. Fig. 13 shows that the PDR of DCR was higher than that of OLSR-mod by more than 0.05 and higher than that of DSDV-mod by more than 0.1. The PDRs became larger as the number of nodes increased. This is because it is more likely to exist available paths, as the number of nodes increased. DCR had a low overhead because the process for routing table configuration was simple, and the information to be exchanged between the nodes was relatively small. A logarithmic scale is adapted in Fig. 14 because the differences among DSDV-mod and other protocols are large. Fig. 14 depicts that DCR and OLSR-mod had very small delays of less than 10 ms. In conclusion, DCR showed the best performance among the three routing algorithms in terms of scalability.

B. EXPERIMENTS FOR DCR PARAMETERS

Experiments with different intervals of 1, 3, and 5 s were conducted to see how the interval of transmitting the NEIGHBORS and HELLO messages affects the performance.

1) COMPARISON OF INTERVALS OF TRANSMITTING NEIGHBORS MESSAGE OVER MAXIMUM SPEED

The interval of varies from 1 s to 5 s. Other simulation parameters are same as the those of IV-A2. Figs. 15 and 16 show the results of DCR for different transmitting intervals of the NEIGHBORS message over maximum speed. Fig. 15 shows that a longer interval leads to a lower PDR. If the interval of transmitting the NEIGHBORS message is 3 s, PDR is lower than that of 1 s by more than 0.02. Meanwhile, if the interval of transmitting the NEIGHBORS message is 5 s, PDR is lower than that of 1 s by more than 0.11. A longer interval of transmitting the NEIGHBORS message makes other nodes recognize the link state of the network much slower. Therefore, it is likely that the routing table does not express the current link state.

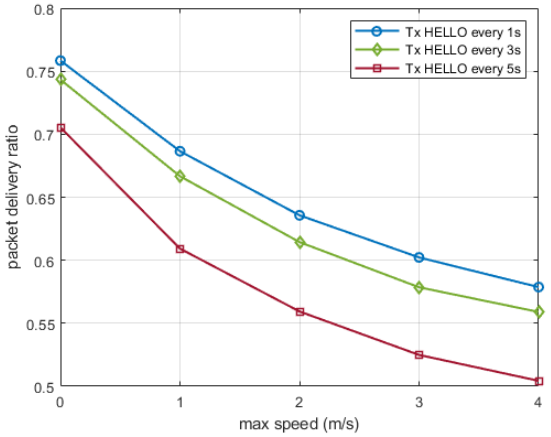

FIGURE 17. PDR for HELLO message interval over maximum speed.

2) COMPARISON FOR INTERVALS OF TRANSMITTING HELLO MESSAGE OVER MAXIMUM SPEED

Figs. 17 and 18 show the performances of DCR for different transmitting intervals of the NEIGHBORS message over maximum speed. Fig. 17 depicts results similar to those in Fig. 15. The PDR decreased with a larger interval of transmitting HELLO message. When the interval of transmitting HELLO message increased, the number of times each node updated the neighbor table decreased. In other words, when a link changes owing to a node dropping out, responding to it takes longer.

The performance evaluation results are as follows: DCR outperformed the other two MANET routing algorithms (i.e., OLSR-mod and DSDV-mod), in terms of the initial

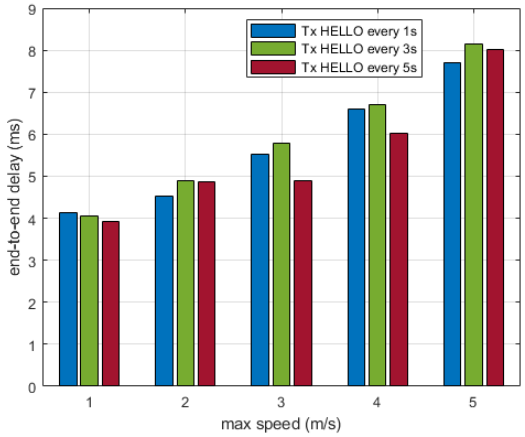

FIGURE 18. **End-to-end delay for HELLO message interval over maximum speed.**

routing-configuration time, PDR, and end-to-end delay. The neighbor table of each node was shared through the sub-GHz band with a large coverage; hence, each node can configure its own routing table fast. The intervals of transmitting the NEIGHBORS and HELLO messages affected the DCR performance. Choosing the right interval is important because a long interval degrades the performance, while a short interval increases the overall network overhead. PDR was particularly sensitive to the interval of transmitting the NEIGHBORS message. Consequently, DCR is suitable for communication of firefighters who rescue people and extinguish fires in an indoor disaster environment.

V. CONCLUSION

This study proposed a MANET location-based routing technique using physical channels for a disaster environment. This algorithm used two channels, namely sub-GHz and 2.4 GHz channels. The data packet and HELLO message were transmitted over the WiFi channel. The link state information is transmitted over the sub-GHz channel. The two-hop routing table was periodically updated based on Dijkstra's algorithm. Our algorithm reflected the link state in real time through the link-cost calculation with SNR. The link state messages were communicated over the sub-GHz channel to reduce the load of control packets and configure the routing table fast. The performance evaluation conducted through the ns-3 simulation tool indicated that the proposed technique outperformed OLSR-mod and DSDV-mod. For the future work, we are going to consider multicasting and broadcasting schemes for the firefighter communication. Another direction is to study the communication not only between firefighters but also between fire engines or fire helicopters which would be challenging.

REFERENCES

[1] K. C. K. Naik, C. Balaswamy, and P. R. Reddy, "Performance analysis of OLSR protocol for MANETs under realistic mobility model," in *Proc. IEEE Int. Conf. Electr., Comput. Commun. Technol. (ICECCT)*, Coimbatore, India, Feb. 2019, pp. 1–5.

[2] S. P. A. Kumar and R. Sachdeva, "Wireless adhoc networks: Performance analysis considerations for AODV routing protocols," in *Proc. 6th Int. Conf. Comput. Sustain. Global Develop. (INDIACom)*, New Delhi, India, Mar. 2019, pp. 140–144.

[3] Y.-B. Ko and N. H. Vaidya, "Location-aided routing (LAR) in mobile ad hoc networks," *Wireless Netw.*, vol. 6, no. 4, pp. 307–321, 2000.

[4] B. Karp and H.-T. Kung, "GPSR: Greedy perimeter stateless routing for wireless networks," in *Proc. 6th Annu. Int. Conf. Mobile Comput. Netw.*, 2000, pp. 243–254.

[5] M. Anand and T. Sasikala, "Efficient energy optimization in mobile ad hoc network (MANET) using better-quality AODV protocol," *Cluster Comput.*, vol. 22, no. S5, pp. 12681–12687, Sep. 2019.

[6] Y. Mostafaei and S. Pashazadeh, "An improved OLSR routing protocol for reducing packet loss ratio in ad-hoc networks," in *Proc. 8th Int. Conf. Inf. Knowl. Technol. (IKT)*, Hamedan, Iran, Sep. 2016, pp. 12–17.

[7] F. A. Al-Zahrani, "On modeling optimizations and enhancing routing protocols for wireless multihop networks," *IEEE Access*, vol. 8, pp. 68953–68973, 2020.

[8] S. Cabrero, X. G. Paneda, D. Melendi, R. Garcia, and T. Plagemann, "Using firefighter mobility traces to understand ad-hoc networks in wildfires," *IEEE Access*, vol. 6, pp. 1331–1341, 2018.

[9] M. Deruyck, J. Wyckmans, L. Martens, and W. Joseph, "Emergency ad-hoc networks by using drone mounted base stations for a disaster scenario," in *Proc. IEEE 12th Int. Conf. Wireless Mobile Comput., Netw. Commun. (WiMob)*, New York, NY, USA, Oct. 2016, pp. 1–7.

[10] M. Y. Arafat and S. Moh, "Location-aided delay tolerant routing protocol in UAV networks for post-disaster operation," *IEEE Access*, vol. 6, pp. 59891–59906, 2018.

[11] M. Del Prete, A. Costanzo, M. Magno, D. Masotti, and L. Benini, "Optimum excitations for a dual-band microwatt wake-up radio," *IEEE Trans. Microw. Theory Techn.*, vol. 64, no. 12, pp. 4731–4739, Dec. 2016.

[12] O. M. Zakaria, A.-H. A. Hashim, W. H. Hassan, O. O. Khalifa, M. Azram, S. Goudarzi, L. B. Jivanadham, and M. Zareei, "State-aware reconfiguration model for multi-radio wireless mesh networks," *KSII Trans. Internet Inf. Syst.*, vol. 11, no. 1, pp. 146–170, 2017.

[13] O. M. Zakaria, A.-H.-A. Hashim, W. H. Hassan, O. O. Khalifa, M. Azram, L. B. Jivanadham, M. L. Sanni, and M. Zareei, "Joint channel assignment and routing in multiradio multichannel wireless mesh networks: Design considerations and approaches," *J. Comput. Netw. Commun.*, vol. 2016, pp. 1–24, Jun. 2016.

[14] U. Raza, P. Kulkarni, and M. Sooriyabandara, "Low power wide area networks: An overview," *IEEE Commun. Surveys Tuts.*, vol. 19, no. 2, pp. 855–873, 2nd Quart., 2017.

[15] N. Sornin, M. Luis, T. Eirich, T. Kramp, and O. Hersent. (2016). *Lorawan Specification*. [Online]. Available: https://lora-alliance.org/sites/default/files/2018-05/lorawan_0_2-20161012_1398_1.pdf

[16] I. Kuzminykh, A. Snihurov, and A. Carlsson, "Testing of communication range in ZigBee technology," in *Proc. 14th Int. Conf. Exper. Designing Appl. CAD Syst. Microelectron. (CADSM)*, Lviv, Ukraine, 2017, pp. 133–136.

[17] T.-N. Do, R. Liu, C. Yuen, M. Zhang, and U.-X. Tan, "Personal dead reckoning using IMU mounted on upper torso and inverted pendulum model," *IEEE Sensors J.*, vol. 16, no. 21, pp. 7600–7608, Nov. 2016.

[18] J.-O. Nilsson, "Infrastructure-free Pedestrian localization," Ph.D. dissertation, KTH Royal Inst. Technol., Stockholm, Sweden, 2013.

[19] C. Chen, P. Zhao, C. X. Lu, W. Wang, A. Markham, and N. Trigoni, "Deep-learning-based pedestrian inertial navigation: Methods, data set, and on-device inference," *IEEE Internet Things J.*, vol. 7, no. 5, pp. 4431–4441, May 2020.

[20] M. Fainberg, "A performance analysis of the ieee 802.11b local area network in the presence of Bluetooth personal area network," M.S. thesis, Dept. Telecommun. Netw., Polytech. Univ., Brooklyn, NY, USA, Jun. 2001.

[21] M. Divya, "Bit error rate performance of BPSK modulation and OFDM-BPSK with Rayleigh multipath channel," *Int. J. Eng. Adv. Technol.*, vol. 2, no. 4, pp. 623–626, Apr. 2013.

[22] S. Sanyal, "Bit error rate performance of QPSK modulation and OFDM-QPSK with AWGN and Rayleigh multipath channel," *Int. J. Sci. Res.*, vol. 4, no. 7, pp. 2086–2088, 2015.

[23] M. Abdullahi, A. Cao, A. Zafar, P. Xiao, and I. A. Hemadeh, "A generalized bit error rate evaluation for index modulation based OFDM system," *IEEE Access*, vol. 8, pp. 70082–70094, 2020.

NAMKYU KIM received the B.S. degree in computer science and engineering from Chung-Ang University, South Korea, in 2019, where he is currently pursuing the M.S. degree in computer science and engineering.

His research interests include mobile *ad hoc* networking, fog/edge computing, and the Internet of Things.

WOONGSOO NA received the B.S., M.S., and Ph.D. degrees in computer science and engineering from Chung-Ang University, Seoul, South Korea, in 2010, 2012, and 2017, respectively.

He was an Adjunct Professor with the School of Information Technology, Sungshin Women's University, Seoul, from 2017 to 2018, and a Senior Researcher with the Electronics and Telecommunications Research Institute, Daejeon, South Korea, from 2018 to 2019. He is currently an Assistant Professor with the Department of Computer Science and Engineering, Kongju National University, Cheonan, South Korea. His current research interests include mobile edge computing, flying *ad hoc* networks, wireless mobile networks, and beyond 5G.

SUNGRAE CHO (Member, IEEE) received the B.S. and M.S. degrees in electronics engineering from Korea University, Seoul, South Korea, in 1992 and 1994, respectively, and the Ph.D. degree in electrical and computer engineering from the Georgia Institute of Technology, Atlanta, GA, USA, in 2002.

He was an Assistant Professor with the Department of Computer Sciences, Georgia Southern University, Statesboro, GA, USA, from 2003 to 2006, and a Senior Member of Technical Staff with the Samsung Advanced Institute of Technology (SAIT), Giheung, South Korea, in 2003. From 1994 to 1996, he was a Research Staff Member with the Electronics and Telecommunications Research Institute (ETRI), Daejeon, South Korea. From 2012 to 2013, he held a Visiting Professorship with the National Institute of Standards and Technology (NIST), Gaithersburg, MD, USA. He is currently a Professor with the School of Computer Science and Engineering, Chung-Ang University (CAU), Seoul. His current research interests include wireless networking, ubiquitous computing, and ICT convergence. He has served for numerous international conferences as the Organizing Committee Chair, such as IEEE SECON, ICOIN, ICTC, ICUFN, TridentCom, and IEEE MASS, and a Program Committee Member for conferences, such as IEEE ICC, MobiApps, SENSORNETS, and WINSYS. He has been a Subject Editor of *IET Electronics Letter*, since 2018. He was an Editor of *Ad Hoc Networks* Journal (Elsevier), from 2012 to 2017.